Creeping Axisymmetric Flow Around a Solid Particle Near a Permeable Obstacle

A. C. Michalopoulou, V. N. Burganos, and A. C. Payatakes
Inst. of Chemical Engineering and High Temperature Chemical Processes and Dept. of Chemical Engineering, University of Patras, GR 261 10 Patras, Greece

The hydrodynamic interaction between a solid particle and a porous obstacle, both of spherical shape, the former moving slowly along the line of their centers and the latter held stationary in an external axisymmetrical flow field, is analyzed. Owing to the linearity of the creeping motion equations and the boundary conditions, this general problem can be decomposed into two simpler problems: I. the motion of the solid sphere relative to the porous one in a fluid at rest; II. an axisymmetrical streaming flow past the two spheres held stationary. The solution to problem II requires further decomposition into the problem of undisturbed flow in the absence of the two spheres and that of the two spheres following each other in a fluid at rest (problem III). The above component flow problems are solved analytically using the stream function formulation in bispherical coordinates. The flow and pressure fields, and the drag forces exerted on both spheres are determined as functions of the permeability, the slip factor, the gap length, and the relative size of the two spheres. In problem I it is found that the drag force exerted on the solid particle increases with decreasing permeability for any value of the gap length. The opposite behavior is observed in problems III (and II). In all cases, however, the drag force exerted on the porous sphere increases as the permeability decreases for any separation distance. In the region of very small separation distances the drag forces on the two spheres in problem I attain a weak maximum at a critical gap length which is a function of the obstacle permeability and the sphere size ratio. The behavior of the drag forces in problems II (and III) is more complicated and depends strongly on the sphere size ratio. The effects of the slip velocity and the particle to streaming velocity ratio (in the composite problem) on the values of the drag forces are also examined.

Introduction

The hydrodynamic interaction between a solid particle and a porous one, or a porous surface, is of great importance in solid-liquid separations and in polymer flow through porous media. In many practical applications, such as sedimentation or deep bed filtration, the way in which particles interact with clusters of other particles, that are formed through coagulation of particles in suspension, or reentrainment of particle deposits, may be crucial for the effectiveness of the overall process. Another important application is cross flow filtration, in which suspended particles move toward a porous surface where they deposit forming a "cake". In this case, the prediction of the deposition rate requires, among other things, the estimation of the hydrodynamic force exerted on the particle as it approaches the porous substrate. In the very important area of polymer flow through porous media, the analysis can be greatly simplified by considering each macromolecule in solution as a porous particle whose trajectory is considerably affected by the presence of solid grains or pore walls in the interior of the porous medium.

Owing to the linearity of the Navier-Stokes equation under creeping flow conditions (Stokes equation) and the boundary and limit conditions, the relatively complex problem of the flow around a solid particle when in the vicinity of a porous surface (and the corresponding pressure field and drag force),

can be obtained by superposing solutions of simpler problems. These component problems refer to the parallel or perpendicular motion of the particle relative to the surface, to the rotation of the particle about an axis parallel or perpendicular to the surface, and to the uniform streaming past the stationary particle. All the aforementioned component problems have been treated by a number of researchers in the past for the special case of solid boundaries (Kynch, 1958; Payne and Pell, 1959; Brenner, 1961; Maude, 1961; Dean and O'Neill, 1963; Goldman et al., 1966; Goldman et al., 1967(a,b); Cooley and O'Neill, 1969 and references therein). However, for the general case of porous boundaries, it is only the normal motion of a solid sphere relative to a porous planar wall and, recently, the rotation of a solid sphere about an axis that is perpendicular to a porous surface (O'Neill and Bhatt, 1991) that have been reported in the literature. Finally, we must also mention the work of Jones (1978) who obtained an approximate solution to the problem of two translating and rotating porous spheres with the method of reflections.

In this article the problem of the normal motion of a solid particle toward or away from a porous obstacle of arbitrary size in an externally applied axisymmetric flow field is analyzed. This general problem can be treated as the result of two component problems, namely, that of the motion of a solid sphere toward a porous one in a fluid which at infinity is at rest (problem I), and that of the two bodies being immersed in an external, axisymmetric streaming flow (problem II), Figure 1a. When the solid particle is sufficiently far from the porous obstacle, the hydrodynamic force exerted on the particle is given by Stokes' law in both cases; however, for finite separation distances, hydrodynamic interaction becomes important and makes it necessary to determine the appropriate correction factor to Stokes' resistance formula.

In the first part of this work we consider the case of a solid sphere moving slowly with constant velocity toward a porous one, along the line passing through their centers in a viscous fluid which far from the two bodies is at rest. Stokes' equation is used to describe the flow in the region between and around the two spheres, and Darcy's law is used to describe the fluid motion in the interior of the porous sphere. The bispherical coordinate system is used to obtain the general solution since it is the natural system to represent the physical boundaries of the problem for any finite separation distance. The solutions in the two flow regions are matched at the porous boundary using continuity of the pressure and of the normal fluid velocity, and the Beavers-Joseph-Saffman slip flow condition. The statement of the problem is completed using the usual kinematical and dynamical boundary conditions on the solid sphere. These boundary conditions will be discussed in detail in the next sections.

The limiting case of the interaction of a solid sphere with an infinitely large porous obstacle is equivalent to the interaction of the solid sphere with a planar porous wall. Closely related problems have already been treated in several previous studies. Goren (1979) studied the normal motion of a solid particle towards a thin, porous membrane that separates a fluid reservoir into two regions. In each region the flow is creeping and the flow through the membrane is assumed to be one-dimensional. The continuity of the normal velocity, which was set proportional to the normal stress difference across the membrane, and zero tangential velocity on either side of the

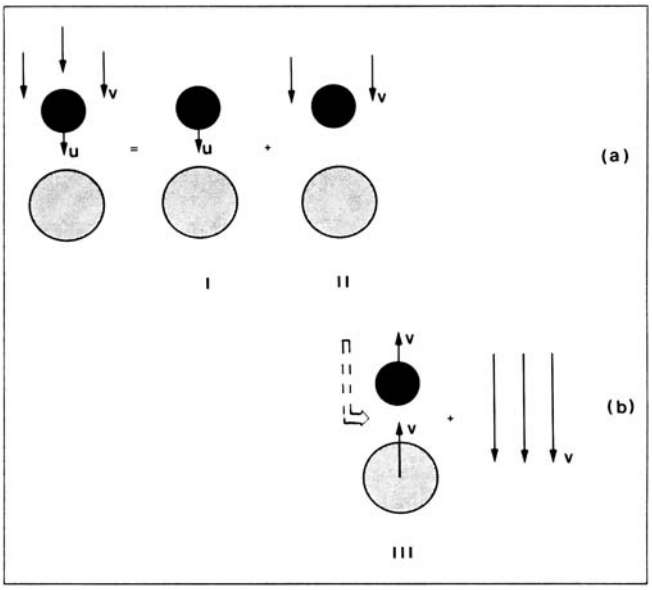

Figure 1. Original and component flow problems.

membrane were used as boundary conditions on the membrane surface. An important conclusion from Goren's work is that the drag force remains finite as the sphere approaches the porous membrane and tends to a value that is a function of the membrane permeability. Goren also observed that as the gap length is varied the drag force attains a maximal value, not necessarily at contact, for large values of the permeability. Since the bispherical coordinate system fails at the limit of the particle touching the plane wall, Goren has estimated the drag force at contact using the lubrication approximation. Nir (1981) solved the same physical problem at zero separation distance, using the same formulation but in the tangent spheres coordinate system. He has calculated the drag force at the limit of low and high membrane permeabilities and agreed with Goren in that the maximal value of the drag force at high permeabilities is not obtained at contact but at a finite separation.

Sherwood (1988) used an approach similar to Nir's but with the addition of the Darcy flow analysis within the porous medium, which was considered as a semi-infinite region. He assumed no slip condition on the porous surface and found that the drag force exerted on the particle at contact remains constant and lower than the Stokes' drag force over a range of high permeabilities, while for small permeability values it increases as the permeability decreases. Recently, O'Neill and Bhatt (1991) used, for the same physical problem, Saffman's slip condition on the porous surface and Darcy's law within the porous wall, but they solved the problem in the case of very low permeability values only, assuming that in this limit the flow in the porous medium can be ignored. In this case, exact solutions for the hydrodynamic correction factor are easily obtained since the system of differential equations that govern the flow inside and outside the porous medium become uncoupled. Thanks to this simplified assumption, O'Neill and Bhatt observed a monotonic increase of the drag force as the solid particle approaches the porous wall, for any permeability value. The "dual" problem, where a porous sphere approaches a solid planar wall, was studied by Payatakes and Dassios (1987) and by Burgauos et al. (1992) and their basic formulation

will be followed here. The corresponding problem of the motion of a porous particle near a plane-fluid interface was analyzed by Yang and Leal (1989), who used Brinkman's law to describe the fluid motion inside the porous sphere and calculated the drag force and torque exerted on the particle via singularity solutions to the Stokes' flow equations of motion.

The second part of this work deals with the case of a solid and a porous sphere immersed in an external axisymmetric streaming flow. This problem can be considered as the result of the superposition of two component problems: that of the undisturbed fluid flow in the absence of the spheres and that of the simultaneous motion of the two spheres, in the same direction, along the line passing through their centers in a fluid which is at rest at infinity (problem III, Figure 1b). The expression for the stream function of the former problem is known while the latter component problem is solved by using a formulation similar to the above but slightly modified boundary conditions on the porous sphere. The drag forces exerted on both the solid particle and the porous obstacle are calculated for a wide range of permeabilities, separations and relative sizes of the two spheres. In the last part of this work, results for the original composite problem are presented using the ratio of the particle velocity to the approach fluid velocity as a parameter. These results are obtained by combination of the results of the two fundamental flow problems analyzed in the first two parts of this work. Solution of these particular component problems (I and II) permits one to obtain the solution to a whole family of related axisymmetric problems by properly chosen superposition. The relevant discussion, along with an interesting application, is presented in the last section.

Motion of a Solid Sphere Towards a Spherical Porous Obstacle (Problem I)

Description and mathematical formulation

Consider a solid sphere of radius α_p moving slowly, with constant velocity, $\boldsymbol{u}$, through an otherwise quiescent, incompressible Newtonian fluid, toward a stationary porous sphere of radius, α_o, as depicted in Figure 2. The instantaneous distance of the solid sphere center from the porous surface is h. All the quantities that will be used here are dimensionless. The basic variables, velocity and length, are rendered dimensionless using the dimensional particle velocity, $\tilde{u} = |\tilde{\boldsymbol{u}}|$, and radius, $\tilde{\alpha}_p$, as characteristic quantities. The pressure is rendered dimensionless using the characteristic quantity $\tilde{\mu}\tilde{u}/\tilde{\alpha}_p$. In the region that is external to both spheres (domain Ω^+), the flow is creeping and is governed by the equations of Stokes and continuity:

$$\nabla P^+ = \nabla^2 \boldsymbol{v}^+$$

$$\nabla \cdot \boldsymbol{v}^+ = 0$$

For axisymmetrical flows a more convenient form of the above equations is obtained by introducing the Stokes' stream function, Ψ^+. In terms of this function, the velocity components in cylindrical coordinates (ρ, z) are:

$$v_\rho^+ = \frac{1}{\rho}\frac{\partial \Psi^+}{\partial z} \quad \text{and} \quad v_z^+ = -\frac{1}{\rho}\frac{\partial \Psi^+}{\partial \rho}$$

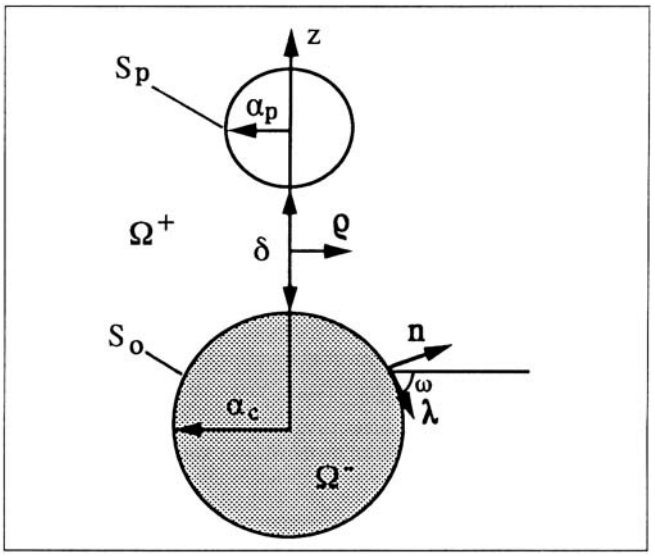

Figure 2. Geometry of the physical problem.

where the superscript $^+$ denotes quantities in Ω^+ (the domain Ω^- is defined as the interior of the porous sphere). Hence, the differential equations governing the flow in Ω^+ are:

$$E^4 \Psi^+ = 0 \tag{1}$$

$$\nabla^2 P^+ = 0 \tag{2}$$

where the operator E^2 in cylindrical coordinates is defined by:

$$E^2 \equiv \rho \frac{\partial}{\partial \rho}\left(\frac{1}{\rho}\frac{\partial}{\partial \rho}\right) + \frac{\partial^2}{\partial z^2}$$

For the determination of the fluid flow in the interior of the porous sphere Darcy's law is used. Darcy's law is an empirical equation and provides a satisfactory representation of the flow in the interior of a statistically homogeneous and isotropic porous material. Discussions on the use of Darcy's law vis à vis that of Brinkman's law to describe flow in porous media are given elsewhere (see, for instance, Neale et al., 1973; Neale and Nader, 1974; Yang and Leal, 1983; O'Neill and Bhatt, 1991). Using Darcy's law the fluid velocity in the interior of the porous sphere is given by:

$$\boldsymbol{v}^- = -k \nabla P^-$$

where $k(=\tilde{k}/\tilde{\alpha}_p^2)$ is the dimensionless permeability of the porous material. Taking the divergence of the above equation and using the continuity equation for the fluid velocity in the porous sphere $(\nabla \cdot \boldsymbol{v}^- = 0)$ we obtain:

$$\nabla^2 P^- = 0 \tag{3}$$

Differential Eqs. 1 in Ω^+ and 3 in Ω^- complemented by an appropriate set of boundary conditions will be solved for the flow and pressure fields in the respective domains. If needed, the pressure field in Ω^+ can subsequently be determined by integrating (along any convenient path in Ω^+) the equation:

$$dP^+ = \frac{\partial P^+}{\partial \rho} d\rho + \frac{\partial P^+}{\partial z} dz \tag{4}$$

The pressure derivatives are calculated from the two components of Stokes' equation that relate the pressure and the stream function in Ω^+ in the following way:

$$\frac{\partial P^+}{\partial \rho} = \frac{1}{\rho} \frac{\partial}{\partial z} (E^2 \Psi^+), \quad \frac{\partial P^+}{\partial z} = -\frac{1}{\rho} \frac{\partial}{\partial \rho} (E^2 \Psi^+) \tag{5}$$

Boundary conditions

The boundary conditions on the solid moving sphere are of two types, kinematical and dynamical (see, for instance, Happel and Brenner, 1963). The kinematical condition describes the impenetrability of the surface of the solid sphere and is expressed as:

$$\Psi^+ = \frac{1}{2} \rho^2 \quad \text{on} \quad S_p \tag{6}$$

The dynamical condition expresses the absence of tangential velocity on the solid surface relative to the sphere and is given by:

$$\frac{\partial \Psi^+}{\partial n} = \rho \frac{\partial \rho}{\partial n} \quad \text{on} \quad S_p \tag{7}$$

where n is distance along the outward normal unit vector $\boldsymbol{n}$ at a point on the surface of the sphere.

On the surface of the stationary porous sphere the following boundary conditions apply:

- Continuity of the pressure across the sphere surface, expressed by:

$$P^+ = P^- \quad \text{on} \quad S_o \tag{8}$$

- Continuity of the normal fluid velocity, expressed by:

$$v_n^+ = v_n^- \quad \text{on} \quad S_o$$

where v_n^+ and v_n^- are the normal velocity components of v^+ and v^-, Figure 2. In terms of the stream function this boundary condition becomes:

$$\frac{1}{\rho} \frac{\partial \Psi^+}{\partial z} \sin\omega - \frac{1}{\rho} \frac{\partial \Psi^+}{\partial \rho} \cos\omega + k \left(\frac{\partial P^-}{\partial z} \cos\omega + \frac{\partial P^-}{\partial \rho} \sin\omega \right) = 0 \tag{9}$$

where ω is such that $\cos\omega = \boldsymbol{\rho} \cdot \boldsymbol{\lambda}$.

- Slip flow condition.

Beavers and Joseph (1967) suggested an *ad hoc* boundary condition for the tangential velocity of a fluid on a permeable boundary, which in our notation is given by:

$$\frac{\partial v_\lambda^+}{\partial n} = \gamma (v_\lambda^+ - v_\lambda^-)$$

where v_λ^+ is the tangential velocity component of v^+ (defined as in Figure 2), and γ is a dimensionless slip factor that is related to the permeability of the porous medium through $\gamma = 1/\lambda_s \sqrt{k}$, where λ_s is a dimensionless constant that characterizes the structure of the porous medium and is determined experimentally. Usually, $0.25 < \lambda_s < 10$ for low porosity consolidated porous media. Experimental validation of the above equation was provided by Beavers and Joseph (1967), Beavers et al. (1970), Taylor (1971), and Richardson (1971). A theoretical justification for this boundary condition is given by Saffman (1971) who, through a statistical treatment of Darcy's law and with standard boundary layer techniques, found that:

$$v_\lambda^+ = \frac{1}{\gamma} \frac{\partial v_\lambda^+}{\partial n} + O(k)$$

In our analysis an extended slip condition is used that assumes that the tangential velocity at a surface point is proportional to the tangential component of the stress tensor prevailing at that point:

$$v_\lambda^+ = -\frac{1}{\gamma} \tau_{n\lambda}^+ \quad \text{on} \quad S_o$$

where $\tau_{n\lambda}^+$ is the tangential fluid stress. In terms of the stream function, the slip condition in cylindrical coordinates has the form:

$$\frac{\partial \Psi^+}{\partial z} \cos\omega + \frac{\partial \Psi^+}{\partial \rho} \sin\omega = \frac{1}{\gamma} \left[\left(2 \frac{\partial^2 \Psi^+}{\partial \rho \partial z} - \frac{1}{\rho} \frac{\partial \Psi^+}{\partial z} \right) \sin 2\omega - \left(\frac{\partial^2 \Psi^+}{\partial \rho^2} - \frac{1}{\rho} \frac{\partial \Psi^+}{\partial \rho} - \frac{\partial^2 \Psi^+}{\partial z^2} \right) \cos 2\omega \right] \tag{10}$$

It should be noted that the use of Darcy's law for the determination of the flow within the porous sphere does not allow one to demand continuity of the shear stress across the porous boundary, which is a natural boundary condition. This is due to the fact that Darcy's law is not of a sufficiently high order to link with the shear stress. The continuity of the shear stress can be satisfied if Brinkman's law is used for the fluid motion in the porous medium. Nevertheless, the use of Darcy's law in combination with the Beavers-Joseph-Saffman slip condition gives a very good representation of the flow near the porous surface provided that the permeability does not take extremely high values (see, for instance, Neale and Nader, 1974).

The following restrictions apply to the stream function, the pressure and their derivatives on the axis:

$$\Psi^+(0, z) = 0, \quad \frac{\partial \Psi^+(0, z)}{\partial z} \text{ finite}, \; P^-(0, z) \text{ finite} \tag{11}$$

Finally, the fact that at infinity the fluid is at rest can be expressed by:

$$\frac{\Psi^+}{\rho^2} \to 0 \quad \text{as} \quad \rho \to \infty \tag{12}$$

Transformation in bispherical coordinates (ξ, μ)

The physical boundaries of this problem suggest the use of the bispherical coordinate system (ξ, μ). The moving solid sphere is characterized by $\xi=\alpha>0$ and the stationary porous one by $\xi=\beta<0$. The relation between cylindrical and bispherical coordinates is given by

$$\rho=\frac{c\sqrt{1-\mu^2}}{\cosh\xi-\mu},\quad z=\frac{c\sinh\xi}{\cosh\xi-\mu}$$

where $c=\sinh\alpha$. Given the ratio of the radii of the two spheres $q(=\tilde{\alpha}_o/\tilde{\alpha}_p)$ and the dimensionless gap length, δ, the three constants that characterize the bispherical coordinate system, c, α, β can be estimated by the following equations:

$$\left.\begin{aligned} c&=\sinh\alpha\\ q&=-\sinh\alpha/\sinh\beta\\ h&=\delta+1=\cosh\alpha+q\cosh\beta-q\end{aligned}\right\}$$

In the limiting case of infinitely large porous sphere (case of planar porous boundary), the bispherical constants are given by:

$$\beta=0,\quad c=\sinh\alpha,\quad \alpha=\ln(h+\sqrt{h^2-1})$$

Equations of motion in (ξ, μ) coordinates

The equations of motion of the fluid in bispherical coordinates are

In Ω^+,

$$E^2(E^2\Psi^+)=0$$

where

$$E^2\equiv\frac{\cosh\xi-\mu}{\sinh^2\alpha}\left[\sinh\xi\,\frac{\partial}{\partial\xi}-(1-\mu^2)\,\frac{\partial}{\partial\mu}+(\cosh\xi-\mu)\,\frac{\partial^2}{\partial\xi^2}+(1-\mu^2)(\cosh\xi-\mu)\,\frac{\partial^2}{\partial\mu^2}\right] \tag{13}$$

with $\xi\in[\beta,\ \alpha]$ and $\mu\in[-1,\ 1]$

In Ω^-

$$\nabla^2P^-=\frac{(\cosh\xi-\mu)}{\sinh^2\alpha}\left[-\sinh\xi\,\frac{\partial P^-}{\partial\xi}+(1-2\mu\cosh\xi+\mu^2)\frac{\partial P^-}{\partial\mu}+(\cosh\xi-\mu)\,\frac{\partial^2P^-}{\partial\xi^2}+(1-\mu^2)(\cosh\xi-\mu)\,\frac{\partial^2P^-}{\partial\mu^2}\right] \tag{14}$$

with $\xi\in(-\infty,\ \beta)$ and $\mu\in[-1,\ 1]$.

Boundary conditions in (ξ, μ) coordinates

The transformed conditions on the solid sphere are:

$$\Psi^+(\alpha,\ \mu)=\frac{1}{2}\,\frac{c^2(1-\mu^2)}{(\cosh\alpha-\mu)^2} \tag{15}$$

$$\frac{\partial\Psi^+(\alpha,\ \mu)}{\partial\xi}=\frac{c^2(1-\mu^2)\sinh\alpha}{(\cosh\alpha-\mu)^3} \tag{16}$$

The transformed conditions on the porous surface are given next. The continuity of pressure, Eq. 8, can be written as:

$$P^+(\beta,\ \mu)=P^-(\beta,\ \mu) \tag{17}$$

In order to eliminate P^+, which does not appear in our differential equations, we differentiate the above equation with respect to μ and combine the result with the transformed form of Eqs. 5 to obtain:

$$c^3\,\frac{\partial P^-}{\partial\mu}=-\frac{(\cosh\xi-\mu)(1-2\cosh^2\xi+\mu\cosh\xi)}{1-\mu^2}\,\frac{\partial\Psi^+}{\partial\xi}-\sinh\xi(\cosh\xi-\mu)\,\frac{\partial\Psi^+}{\partial\mu}+\frac{3\sinh\xi(\cosh\xi-\mu)^2}{1-\mu^2}\,\frac{\partial^2\Psi^+}{\partial\xi^2}+2\sinh\xi(\cosh\xi-\mu)^2\,\frac{\partial^2\Psi^+}{\partial\mu^2}-(\cosh\xi-\mu)^2\,\frac{\partial^2\Psi^+}{\partial\xi\partial\mu}+\frac{(\cosh\xi-\mu)^3}{1-\mu^2}\,\frac{\partial^3\Psi^+}{\partial\xi^3}+(\cosh\xi-\mu)^3\,\frac{\partial^3\Psi^+}{\partial\mu^2\partial\xi} \tag{18}$$

at $\xi=\beta$.

This operation has the consequence that P^+ can be determined, by integrating Eq. 4, only within a constant. This causes no problem, as only the pressure gradient is of interest here. Besides, at the end, one can always set the constant to the value that will satisfy Eq. 17.

The transformed equation for the continuity of the normal fluid velocity, Eq. 9, is

$$\frac{1}{c}\,(\cosh\beta-\mu)\,\frac{\partial\Psi^+(\beta,\ \mu)}{\partial\mu}-k\,\frac{\partial P^-(\beta,\ \mu)}{\partial\xi}=0 \tag{19}$$

whereas the transformed slip condition is given by:

$$(\gamma c-3\sinh\beta)\,\frac{\partial\Psi^+(\beta,\ \mu)}{\partial\xi}-3(1-\mu^2)\,\frac{\partial\Psi^+(\beta,\ \mu)}{\partial\mu}-(\cosh\beta-\mu)\,\frac{\partial^2\Psi^+(\beta,\ \mu)}{\partial\xi^2}+(1-\mu^2)(\cosh\beta-\mu)\times\frac{\partial^2\Psi^+(\beta,\ \mu)}{\partial\mu^2}=0 \tag{20}$$

The boundary conditions on the axis become:

$$\Psi^+(\xi,\ \pm1)=0 \tag{21}$$

$$\frac{\partial\Psi^+(\xi,\ \pm1)}{\partial\mu},\ P^-(\xi,\ \pm1),\quad \text{finite} \tag{22}$$

Finally, we must have $\Psi^+\to0$ at infinity.

Solution

The general solution of the partial differential equations that govern the flow in Ω^+ (Eq. 13) and in Ω^- (Eq. 14) can be

obtained by the R-separation method. Stimson and Jeffery (1926) have shown that the general solution for the stream function is given by:

$$\Psi^{+}(\xi, \mu) = (\cosh\xi - \mu)^{-3/2} \sum_{n=1}^{\infty} \mathcal{W}_n(\xi) \mathcal{G}_{n+1}(\mu) \qquad (23)$$

where

$$\mathcal{W}_n(\xi) = a_n e^{(n-1/2)\xi} + b_n e^{-(n-1/2)\xi} + c_n e^{(n+3/2)\xi} + d_n e^{-(n+3/2)\xi} \qquad (24)$$

and

$$\mathcal{G}_{n+1}(\mu) = \frac{1}{(2n+1)} [P_{n-1}(\mu) - P_{n+1}(\mu)]$$

$\mathcal{G}_{n+1}(\mu)$ is the Gegenbauer polynomial of the first kind, of order $(n+1)$ and degree $(-1/2)$. Expression 23 satisfies the requirement that the stream function be zero at infinity and on the axis, and the boundary conditions expressed by Eq. 22.

The general solution for the pressure in Ω^{-} can be expressed as a series expansion in terms of Legendre polynomials:

$$P^{-}(\xi, \mu) = (\cosh\xi - \mu)^{1/2} \sum_{n=0}^{\infty} \mathcal{V}_n(\xi) P_n(\mu) \qquad (25)$$

where

$$\mathcal{V}_n(\xi) = e_n e^{(n+1/2)\xi} \qquad (26)$$

$P_n(\mu)$ is the Legendre polynomial of the first kind, of order n and degree 0. Legendre polynomials of the second kind $Q_n^m(\mu)$ are omitted in Eq. 23 and in Eq. 25 because they diverge as $\mu \to 1$, which violates Eqs. 21 and 22.

The integration constants a_n, b_n, c_n, d_n, e_n are estimated using the boundary conditions described in the previous section. Inserting the general solution for the stream function into the boundary conditions, Eqs. 15 and 16, for the solid sphere we obtain, following Brenner (1961):

$$\mathcal{W}_n(\alpha) = \frac{c^2\sqrt{2}}{2} n(n+1) \left[\frac{e^{-(n-1/2)\alpha}}{2n-1} - \frac{e^{-(n+3/2)\alpha}}{2n+3} \right] \qquad n = 1,2,3,\ldots \qquad (27)$$

and

$$\mathcal{W}_n'(\alpha) = -\frac{\sqrt{2}}{4} c^2 n(n+1) [e^{-(n-1/2)\alpha} - e^{-(n+3/2)\alpha}] \qquad n = 1,2,3,\ldots \qquad (28)$$

respectively. The prime in the above equation denotes differentiation with respect to ξ. Substituting the general solutions for the stream function and the pressure in the last three boundary conditions (Eqs. 18-20), collecting the $\mu^m \mathcal{G}_{m+1}(\mu)$ and $\mu^m P_m(\mu)$ terms $(m = 0, \ldots, \kappa)$, and using properties of the Legendre and Gegenbauer polynomials (see, for instance, Hobson, 1965) one can cast after lengthy manipulations the boundary conditions in the following form:

$$\sum_{j=-\kappa}^{\kappa} \sum_{n=0 \text{ or } 1}^{\infty} x_{j+\kappa+n}(\beta) P_{n+j}(\mu) = 0 \qquad (29)$$

where $x_i(\beta)$ are linear combinations of the unknown coefficients. Using, now, the orthogonality of the Legendre polynomials we obtain a set of algebraic equations which along with Eqs. 27 and 28 can be solved for the expansion coefficients. Despite the use of a very concise formulation, the final form of these algebraic equations is quite complicated; the interested reader is referred to Appendix A. Truncating the series solution at $n = N$ we can solve numerically for the unknown expansion coefficients and obtain results for the flow and the pressure field in the exterior and in the interior of the porous sphere. Since $\kappa \neq 0$ in Eq. 29, we had to use sufficiently high N to ensure negligible contribution to the solution of the extra unknowns a_{N+1}, ..., $a_{N+\kappa}$, ..., b_{N+1}, ..., $b_{N+\kappa}$ and so on. The selection of the truncation number depends on the required accuracy of the results and on the speed of convergence of the solution series. For small and moderate permeability values $(k < 10^{-2})$ $N = 3$ to 5 was sufficient even for small separations, while for large permeabilities $(k > 10^{-2})$ and small gap lengths $(\delta < 0.1)$ large truncation numbers (100 to 150) had to be used for satisfactory convergence.

Streamlines and isobars

Samples of streamlines in Ω^{+} and isobars in Ω^{-} for a typical case are shown in Figure 3. The reported pressure values are the relative pressures $P^{-}(\xi, \mu) - P^{-}(-\infty, \mu)$, where $P^{-}(-\infty, \mu) = \sqrt{2}/2\, e_0$ is the pressure at the pole $(-\infty, \mu)$ in the interior of the porous sphere. The porous sphere, which in this example is twice as large as the solid one and has a relatively large permeability $(k = 0.1)$, is stationary and very close to the solid one. The motion of the fluid is caused solely by the motion of the solid sphere. As it was expected, the streamlines in the exterior of the two spheres and the isobars inside the porous

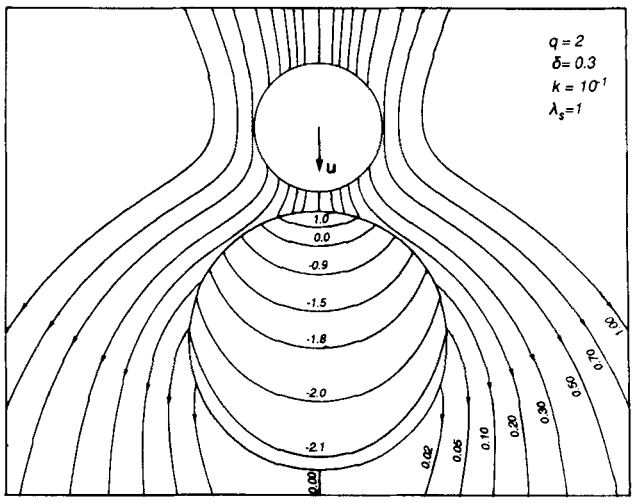

Figure 3. Streamlines and isobars during the motion of a solid sphere toward a porous one in a fluid at rest.

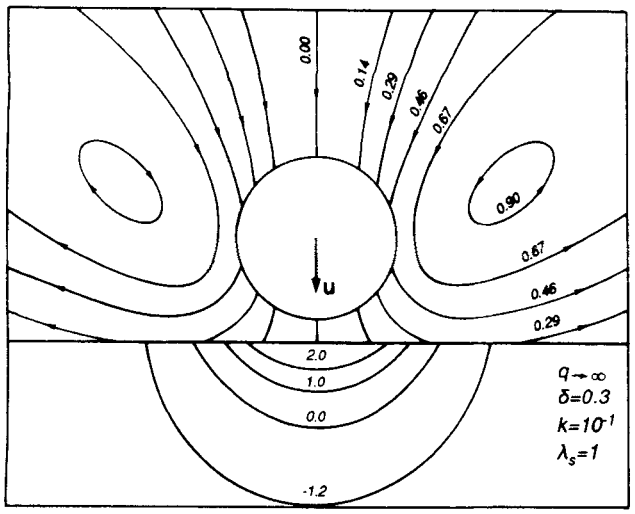

Figure 4. Streamlines and isobars during the normal motion of a solid sphere towards a planar porous wall.

sphere are symmetric about the line of centers of the two spheres. As the solid sphere approaches the porous one the fluid between them is forced to flow both through and around the porous sphere. It is also noteworthy that in Figure 3 the streamlines intercept the porous sphere obliquely due to the existence of the slip velocity on the porous surface ($\lambda_s = 1$).

For an infinitely large porous sphere ($q \to \infty$) the shape of the streamlines in Ω^+ looks quite different from that in the case of finitely sized obstacles for the same permeability and gap length. This limiting case, where the solid sphere moves towards an almost planar porous wall, is depicted in Figure 4. As the solid sphere approaches the wall a large amount of fluid prefers to enter the porous medium than to slip on it mainly thanks to the zero curvature of the surface. It is also interesting to note the formation of quasi-stationary vortices in Ω^+.

Calculation of the drag forces

The drag force exerted by the fluid on both the solid particle and the porous obstacle can be obtained by integrating the tangential fluid stress and the pressure on their surfaces. Following Stimson and Jeffery (1926) the dimensional drag force is given by:

$$\tilde{F}_D = \pi\tilde{\mu}\tilde{\alpha}_p\tilde{u}\int_S \rho^3 \frac{\partial}{\partial n}\left(\frac{E^2\Psi^+}{\rho^2}\right) ds \tag{30}$$

where the integral is taken along a meridian S of the sphere in a sense which is right-handedly related to $\boldsymbol{n}$. This is a quite general expression and can be applied to steady creeping flows even for bounded fluids and for any kind of conditions applying on the boundaries (Happel and Brenner, 1963). Substituting Eq. 13 in Eq. 30 and using certain properties of the Legendre polynomials, Stimson and Jeffery (1926) arrived at a more practical form of the drag force expression which in our notation is:

$$f_p = \frac{\tilde{F}_p}{6\pi\tilde{\mu}\tilde{\alpha}_p\tilde{u}} = \frac{2\sqrt{2}}{3\sinh\alpha}\sum_{n=1}^{\infty}(a_n + c_n) \tag{31}$$

for the solid particle, whereas for the porous obstacle the corresponding expression is:

$$f_o = \frac{\tilde{F}_o}{6\pi\tilde{\mu}\tilde{\alpha}_o\tilde{u}} = \frac{2\sqrt{2}}{3\sinh\alpha}\frac{\tilde{\alpha}_p}{\tilde{\alpha}_o}\sum_{n=1}^{\infty}(b_n + d_n) \tag{32}$$

Both drag forces are rendered dimensionless using the Stokes' force as reference. These dimensionless drag forces, f_p and f_o, depend on the permeability, k, of the porous sphere, the gap length, δ, the sphere size ratio, q, and the slip coefficient γ. Typical values of the dimensionless permeability k, lie in the range (0, 1) which corresponds approximately to porosities in the range (0, 0.85). In Table 1 values of the drag forces exerted on the solid particle, f_p, and on the porous obstacle, f_o, are presented for equally sized spheres ($q = 1$). The two drag forces have opposite directions but exhibit qualitatively similar behavior with the gap length and the permeability. Note that drag force results for small separations and large permeabilities should be regarded with some reservation. An order of magnitude analysis shows that values of δ smaller than $\sqrt{k}$ are comparable to the pore size of some types of porous media. In such cases, accurate determination of the drag forces on the two bodies would require a detailed flow analysis at the pore scale using a reliable model of the pore structure.

Table 1. Dimensionless Drag Forces for the Solid and Porous Spheres ($q = 1$, $\lambda_s = 1$)

	$k=0$		$k=10^{-3}$		$k=10^{-2}$		$k=10^{-1}$		$k=1$	
δ	f_p	f_o	f_p	f_o	f_p	f_o	f_p	f_o	f_p	f_o
50	1.0008	0.0289	1.0008	0.0280	1.0008	0.0265	1.0006	0.0225	1.0003	0.0115
20	1.0047	0.0684	1.0045	0.0664	1.0043	0.0627	1.0036	0.0533	1.0019	0.0272
10	1.0159	0.1264	1.0154	0.1227	1.0146	0.1159	1.0123	0.0982	1.0062	0.0496
5	1.0485	0.2220	1.0470	0.2152	1.0442	0.2030	1.0369	0.1711	1.0178	0.0837
2	1.1695	0.4272	1.1629	0.4126	1.1511	0.3863	1.1207	0.3180	1.0500	0.1383
1	1.3685	0.6702	1.3499	0.6418	1.3167	0.5911	1.2344	0.4628	1.0770	0.1685
0.75	1.4919	0.8060	1.4632	0.7669	1.4123	0.6977	1.2907	0.5277	1.0842	0.1747
0.50	1.7226	1.0497	1.6691	0.9850	1.5754	0.8723	1.3714	0.6172	1.0889	0.1777
0.25	2.3477	1.6883	2.1828	1.5116	1.9162	1.2256	1.4874	0.7431	1.0879	0.1752
0.10	4.0318	3.3809	3.2182	2.5552	2.3463	1.6645	1.5732	0.8357	1.0842	0.1713
0.05	6.6786	6.0305	4.0634	3.4033	2.5519	1.8736	1.6035	0.8683	1.0829	0.1700
0.01	27.008	26.363	5.1001	4.4425	2.7382	2.0626	1.6284	0.8952	1.0820	0.1690

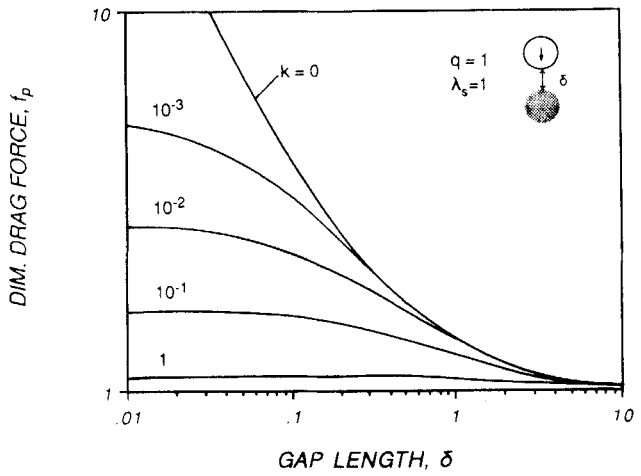

Figure 5. Variation of the dimensionless drag force on the solid particle with the gap length for several permeabilities (problem I).

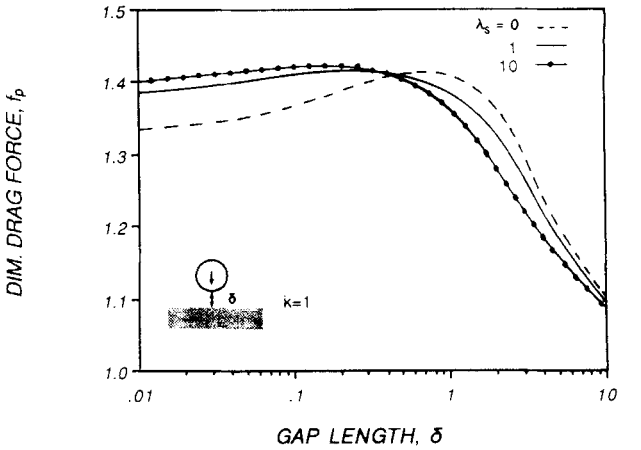

Figure 7. Slip flow effects on the dimensionless drag force exerted on a solid particle approaching a planar porous obstacle ($q \to \infty$).

Figure 5 shows the dependence of the drag force exerted on the solid particle on the gap length for several permeability values. It is clear that for moderate and high permeabilities the drag force tends to an almost constant value at small separations. For zero permeability the drag force increases rapidly as the gas length goes to zero and our results in this case are in good agreement with Cooley and O'Neill (1969). For high permeability values a weak maximum appears as the gap length decreases (which can be seen more clearly in Table 1 for $k = 1$).

The effect of the slip velocity on the drag force is very important as seen in Figure 6. It was pointed out above that the slip coefficient, γ, depends on the permeability and the dimensionless parameter λ_s that characterizes the porous medium. In Figure 6 we study the effect of variable γ on the drag force exerted on the solid particle as induced solely by changes in λ_s, that is, for constant permeability. Note that higher values for the drag force are obtained if the slip velocity on the porous surface is neglected. The drag force decreases as the slip coefficient increases for any gap length value. The same monotonic behavior was observed for any permeability value in the range (0, 1). Similar observations can be made for the force exerted on the porous sphere but on a different magnitude scale (the values obtained for the drag force are smaller). For infinitely large porous obstacles an interesting behavior of the drag force exerted on the solid sphere is obtained as the slip coefficient changes (Figure 7). For large separations, as the slip coefficient increases the drag force exerted on the solid sphere decreases monotonically as in the previous case of equal spheres. However, below a critical gap length the drag force decreases as δ decreases. This indicates that at small separations and for sufficiently high permeabilities the fluid prefers to flow through the porous medium rather than to slip on its surface.

The effect of the sphere size ratio on the drag force exerted on the solid sphere is shown in Figure 8. As the sphere size ratio, q, increases, the drag force also increases for all the gap lengths due to the increased resistance to the fluid flow by the

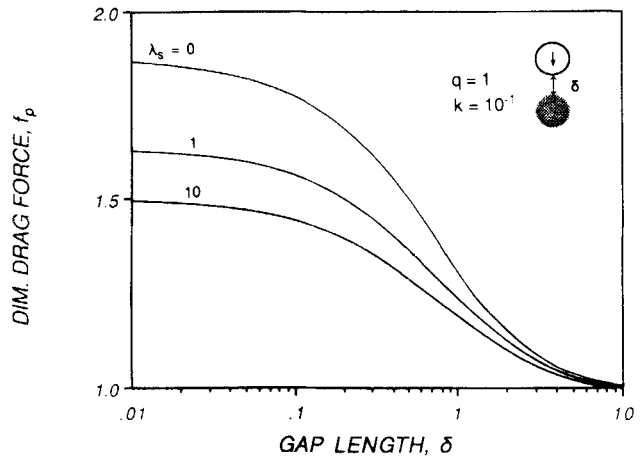

Figure 6. Slip flow effects on the dimensionless drag force exerted on a solid particle approaching a porous obstacle ($q = 1$).

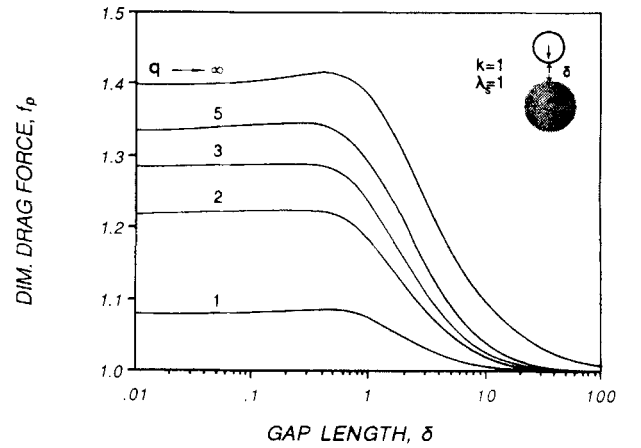

Figure 8. Dependence of the dimensionless drag force exerted on a solid particle approaching a porous obstacle on the gap length: variation with the sphere size ratio.

Table 2. Dimensionless Drag Force for the Solid Sphere ($q \to \infty$, $\lambda_s = 1$)

δ	$k=0$	$k=10^{-3}$	$k=10^{-2}$	$k=10^{-1}$	$k=1$
50	1.0226	1.0225	1.0225	1.0224	1.0221
20	1.0565	1.0565	1.0563	1.0556	1.0536
10	1.1135	1.1131	1.1124	1.1098	1.1014
5	1.2279	1.2264	1.2233	1.2129	1.1797
2	1.6962	1.5602	1.5405	1.4770	1.3141
1	2.1255	2.0905	2.0136	1.7880	1.3906
0.75	2.4893	2.4277	2.2933	1.9307	1.4074
0.50	3.2054	3.0685	2.7775	2.1210	1.4176
0.25	5.3052	4.7621	3.7682	2.3646	1.4151
0.10	11.459	8.1754	4.8903	2.5248	1.4048
0.05	21.586	10.702	5.3744	2.5772	1.4000
0.01	101.90	13.498	5.7910	2.6177	1.39_6*

*Use of a small character indicates the the last digit may change if additional terms of the series solution (Eqs. 31 and 32) are included (large values of N).

obstacle. Note, also, that the drag force increases quickly with q in the lower range of q values ($q=1$ to $q=2$) whereas above the value $q=5$ the drag force undergoes a slight change only. Similar results were obtained for all the permeabilities examined.

Finally, it is worthwhile paying particular attention to the case of a solid particle moving towards (or away from) a planar porous wall, a case that has attracted the interest of several investigators. The drag force values for the solid particle are presented in Table 2 and have resulted from consideration of both slip flow and flow inside the wall. The drag force for small and moderate permeabilities increases as the gap length decreases but for high permeabilities a maximum value of the drag force is obtained at a finite separation. As it can be seen the drag force values in Table 2 agree with Brenner (1961) for $k=0$. If the internal motion of the fluid had been neglected (O'Neill and Bhatt, 1991), higher drag forces would have been obtained, as it is shown in Figure 9. The error in neglecting the flow through the porous medium appears very significant, even for moderate permeabilities, tending obviously to nil as the permeability goes to nil.

Axisymmetrical Flow Past One Solid and One Porous Sphere at Rest: Problem II

Description of the problem

Consider the case of a solid and a porous sphere held stationary in an axisymmetrical streaming flow with approach velocity $\bar{v}$, used as reference velocity in this section (Figure 1a). The fluid motion is described by the creeping motion equations in the exterior and Darcy's law in the interior of the porous sphere as in the previous problem, but the general solution for the stream function (Eq. 23) is no longer valid since it fails to satisfy the boundary condition for the fluid motion at infinity. This problem could be circumvented by adding to this general solution the stream function that would pertain in the absence of the solid sphere. This method has been followed by Goren and O'Neill (1971) in the case of a stationary solid sphere exposed to uniform streaming in the vicinity of a solid wall. However, in the present problem, this would lead to a quite complicated formulation for the general solution and the boundary conditions due to the existence of the finitely sized, porous sphere. A more attractive method was devised here, based on the superposition of the flow problems depicted in Figure 1b: that of the undisturbed fluid flow in the absence of the two spheres, and that of the simultaneous motion of the two spheres along the line passing through their centers in a fluid which at infinity is at rest (problem III). Problems II and III give the same results for the drag forces acting on both spheres and the same values for the isobars in the interior of the porous sphere, since the contribution of the uniform flow to the pressure and viscous stresses is nil. The solution to the undisturbed flow problem is straightforward, expressed by:

$$\Psi^* = \frac{1}{2}\rho^2$$

for the stream function in cylindrical coordinates. The solution to problem III is given below.

Simultaneous Motion of the Two Spheres Through an Otherwise Immobile Fluid: Problem III

In this section we consider the case where the two spheres (one solid and one porous) move slowly along the line passing through their centers at equal velocities, v, in a fluid which at

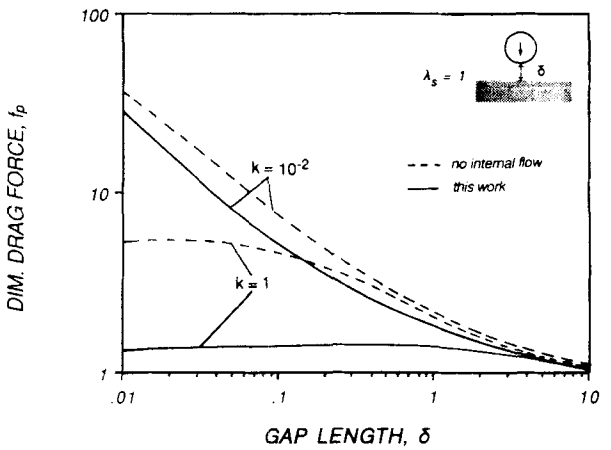

Figure 9. Drag force on a solid particle approaching a planar porous wall vs. separation distance for two permeability values (continuous lines).

Comparison with the approximation of neglecting the internal motion (dashed lines).

infinity is at rest (Figure 1b). The flow is induced by the motion of the two spheres and is governed by the creeping flow equations in the exterior and Darcy's law in the interior of the porous sphere. Obviously, the conditions on the surface of the solid sphere remain the same as in problem I (Eqs. 6 and 7) with a sign change on the RHS since the particle moves in the positive z-direction in this case. The conditions on the porous surface, however, must be modified in order to include the effect of the motion of the sphere on the continuity of the normal velocity and on the slip tangential velocity. Hence, for the problem under consideration the continuity of the normal velocity can be expressed as:

$$v_n^+ - v_n^- = \cos\omega \quad \text{on} \quad S_o$$

which in bispherical coordinates becomes:

$$\frac{1}{c^2}(\cosh\beta-\mu)^2\frac{\partial\Psi^+(\beta,\mu)}{\partial\mu}-\frac{1}{c}k(\cosh\beta-\mu)\frac{\partial P^-}{\partial\xi} = -\frac{1-\mu\cosh\beta}{\cosh\beta-\mu} \quad (33)$$

Taking into account the motion of the porous sphere, the slip velocity on the porous surface can be expressed as:

$$v_\lambda^+ + \sin\omega = \frac{1}{\gamma}\tau_{n\lambda}^+$$

and in bispherical coordinates as:

$$(\cosh\beta-\mu)^3(\gamma c-3\sinh\beta)\frac{\partial\Psi^+}{\partial\xi} - 3(1-\mu^2)(\cosh\beta-\mu)^3\frac{\partial\Psi^+}{\partial\mu}-(\cosh\beta-\mu)^4\frac{\partial^2\Psi^+}{\partial\xi^2} + (1-\mu^2)(\cosh\beta-\mu)^4\frac{\partial^2\Psi^+}{\partial\mu^2}=\gamma c^3(1-\mu^2)\sinh\beta \quad (34)$$

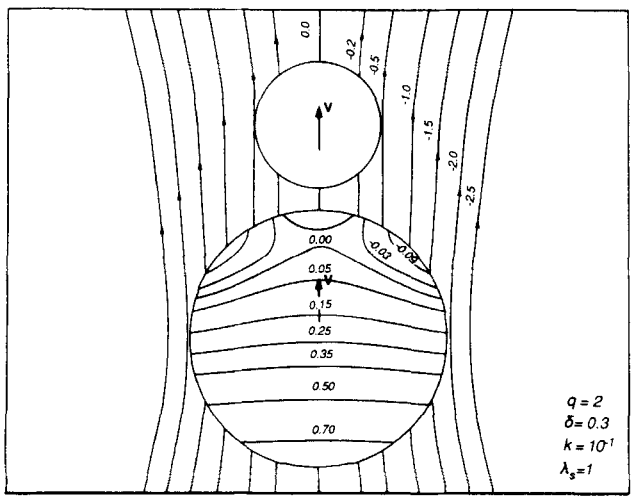

Figure 10. Streamlines and isobars during simultaneous motion of a solid and a porous sphere in a fluid at rest.

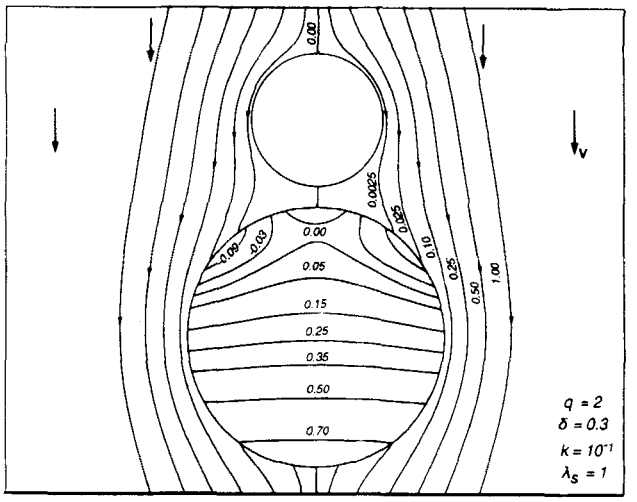

Figure 11. Streamlines and isobars in the case of a solid and a porous sphere immersed in an external uniform flow.

The right hand side of Eqs. 33 and 34 must be expressed as a series expansion of Legendre or Gegenbauer polynomials. This can be done using the relation (Morse and Feshbach, 1950):

$$(\cosh\xi-\mu)^{-1/2}=\sqrt{2}\sum_{m=0}^{\infty}e^{-(m+1/2)|\xi|}P_m(\mu)$$

Introducing the general solutions for the stream function Ψ^+ and the pressure P^- in the expressions, Eqs. 33 and 34, one obtains, after quite lengthy manipulations, a set of linear algebraic equations for the unknown coefficients a_n, b_n, c_n, d_n and e_n. The interested reader can find these equations in Appendix B. The rest of the equations needed for the determination of the unknown coefficients can be obtained from the boundary conditions that hold on the solid sphere and from the continuity of the derivative of the pressure on the porous

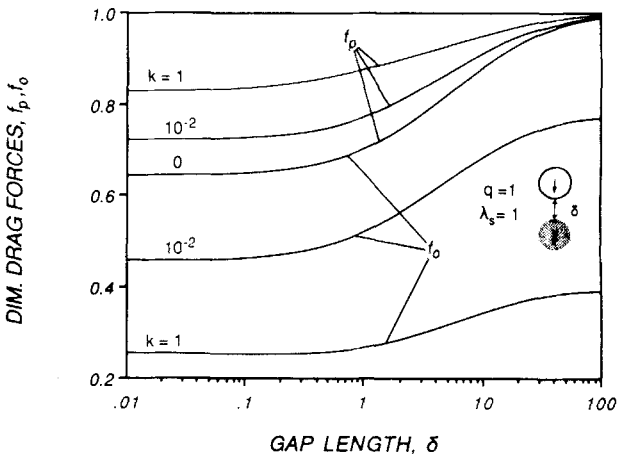

Figure 12. Variation of the dimensionless drag forces on the solid and on the porous sphere with the gap length for various permeabilities (problem III).

Table 3. Dim. Drag Forces for the Solid and the Porous Sphere ($\lambda_s = 1$)

δ \ k	f_p					f_o					q
	0	10^{-3}	10^{-2}	10^{-1}	1	0	10^{-3}	10^{-2}	10^{-1}	1	
50	0.9815	0.9820	0.9830	0.9856	0.9926	0.7611	0.7385	0.6978	0.5926	0.3033	
20	0.9745	0.9752	0.9766	0.9802	0.9899	0.5473	0.5308	0.5010	0.4243	0.2157	
10	0.9761	0.9768	0.9782	0.9816	0.9907	0.3640	0.3526	0.3320	0.2796	0.1406	
5	0.9826	0.9832	0.9842	0.9868	0.9934	0.2158	0.2084	0.1953	0.1627	0.0807	
2	0.9904	0.9907	0.9914	0.9929	0.9965	0.1062	0.1020	0.0946	0.0771	0.0383	
1	0.9934	0.9938	0.9942	0.9953	0.9976	0.0696	0.0665	0.0612	0.0492	0.0251	0.1
0.75	0.9942	0.9945	0.9950	0.9959	0.9979	0.0609	0.0580	0.0532	0.0426	0.0221	
0.50	0.9950	0.9953	0.9956	0.9965	0.9981	0.0524	0.0498	0.0456	0.0364	0.0192	
0.25	0.9957	0.9959	0.9963	0.9970	0.9984	0.0442	0.0419	0.0382	0.0306	0.0164	
0.10	0.9967	0.99_6	0.99_6	0.99_6	0.99_8	0.0395	0.0374	0.0341	0.0269	0.0147	
50	0.9733	0.9741	0.9755	0.9792	0.9893	0.9449	0.9171	0.8668	0.7366	0.3776	
20	0.9430	0.9447	0.9477	0.9298	0.9773	0.8775	0.8515	0.8044	0.6146	0.3493	
10	0.9096	0.9123	0.9172	0.9046	0.9643	0.7930	0.7690	0.7258	0.5251	0.3127	
5	0.8763	0.8801	0.8870	0.8886	0.9518	0.6848	0.6631	0.6241	0.4060	0.2646	
2	0.8537	0.8586	0.8673	0.8895	0.9432	0.5451	0.5255	0.4908	0.3408	0.2037	
1.0	0.8532	0.8586	0.8678	0.8910	0.9415	0.4693	0.4504	0.4176	0.3216	0.1748	0.5
0.75	0.8548	0.8602	0.8696	0.8934	0.9412	0.4465	0.4278	0.3957	0.3011	0.1673	
0.50	0.8573	0.8629	0.8723	0.8967	0.9409	0.4217	0.4033	0.3720	0.2791	0.1596	
0.25	0.8610	0.8667	0.8760	0.8994	0.9409	0.3946	0.3765	0.3465	0.2647	0.1516	
0.10	0.8640	0.8697	0.8787	0.9005	0.9414	0.3770	0.3593	0.3303	0.2597	0.1447	
50	0.9720	0.9728	0.9743	0.9781	0.9889	0.9720	0.9434	0.8917	0.7578	0.3886	
20	0.9363	0.9381	0.9415	0.9503	0.9746	0.9363	0.9086	0.8586	0.7293	0.3735	
10	0.8895	0.8928	0.8987	0.9140	0.9561	0.8895	0.8629	0.8149	0.6912	0.3529	
5	0.8265	0.8317	0.8412	0.8655	0.9317	0.8265	0.8010	0.7552	0.6378	0.3236	
2	0.7425	0.7503	0.7647	0.8011	0.8986	0.7425	0.7171	0.6723	0.5607	0.2831	
1	0.6983	0.7081	0.7253	0.7674	0.8769	0.6983	0.6724	0.6267	0.5166	0.2651	1.0
0.75	0.6859	0.6963	0.7143	0.7577	0.8686	0.6859	0.6596	0.6135	0.5038	0.2617	
0.50	0.6729	0.6840	0.7028	0.7472	0.8583	0.6729	0.6461	0.5996	0.4905	0.2596	
0.25	0.6593	0.6712	0.6905	0.7362	0.8453	0.6593	0.6319	0.5854	0.4767	0.2588	
0.10	0.6509	0.6631	0.6824	0.7297	0.8363	0.6509	0.6324	0.5770	0.4678	0.2591	
50	0.9449	0.9458	0.9474	0.9517	0.9633	0.9733	0.9584	0.9296	0.8546	0.6485	
20	0.8775	0.8794	0.8830	0.8924	0.9185	0.9430	0.9285	0.9004	0.8273	0.6269	
10	0.7930	0.7962	0.8023	0.8183	0.8625	0.9096	0.8954	0.8678	0.7962	0.6013	
5	0.6848	0.6897	0.6691	0.7235	0.7911	0.8763	0.8620	0.8343	0.7629	0.5720	
2	0.5451	0.5521	0.5655	0.5998	0.6960	0.8537	0.8385	0.8092	0.7347	0.5432	
1	0.4693	0.4773	0.4926	0.5303	0.6386	0.8532	0.8372	0.8065	0.7293	0.5351	2.0
0.75	0.4465	0.4548	0.4706	0.5087	0.6199	0.8548	0.8385	0.8073	0.7295	0.5342	
0.50	0.4217	0.4303	0.4464	0.4846	0.5989	0.8573	0.8407	0.8091	0.7307	0.5340	
0.25	0.3946	0.4035	0.4196	0.4578	0.5755	0.8610	0.8442	0.8123	0.7332	0.5345	
0.10	0.3770	0.3860	0.4017	0.4404	0.5603	0.8640	0.8470	0.8151	0.7353	0.5353	
50	0.7611	0.7618	0.7634	0.7680	0.7806	0.9815	0.9784	0.9718	0.9524	0.9000	
20	0.5473	0.5487	0.5515	0.5599	0.5830	0.9745	0.9713	0.9648	0.9452	0.8924	
10	0.3640	0.3657	0.3694	0.3803	0.4105	0.9761	0.9729	0.9662	0.9462	0.8924	
5	0.2158	0.2176	0.2215	0.2332	0.2660	0.9826	0.9794	0.9725	0.9552	0.8973	
2	0.1062	0.1078	0.1113	0.1216	0.1508	0.9904	0.9871	0.9802	0.9597	0.9045	
1	0.0696	0.0711	0.0741	0.0827	0.1080	0.9934	0.9901	0.9833	0.9629	0.9078	10.0
0.75	0.0609	0.0622	0.0651	0.0731	0.0973	0.9942	0.9910	0.9841	0.9638	0.9086	
0.50	0.0524	0.0537	0.0563	0.0636	0.0866	0.9950	0.9918	0.9849	0.9646	0.9095	
0.25	0.0442	0.0454	0.0477	0.0543	0.0763	0.9957	0.992_2	0.985_6	0.965_2	0.91_0	
0.10	0.0394	0.0422	0.04_4	0.0498	0.0714	0.99_7	0.99_2	0.98_5	0.96_0	0.9	

surface (Appendix A). The resulting linear algebraic system is solved numerically following the procedure described earlier.

Typical streamlines and isobars for the simultaneous motion of the two spheres in a fluid which at infinity is at rest are shown in Figure 10. Again, relative pressure values are reported, using the pressure at the pole $(-\infty, \mu)$ as reference. The illustration refers to the case of a porous sphere twice as large as the solid one, of relatively high permeability and at small separation distance. It is seen that the streamlines are almost parallel to the axis due to the high value of the permeability. Superposing a uniform flow onto these results we can obtain the streamlines and the isobars for the case of two spheres immersed in an external uniform flow. The flow pattern and the pressure field for this case are presented in Figure 11. In this plot we notice that the streamlines around the two spheres are more curved than in Figure 10, whereas the pressure field is not affected by the uniform field, following our superposition. Notice also that in both Figures 10 and 11 the streamlines do not intercept the porous sphere at right angles due to the existence of the tangential slip velocity.

The dimensionless drag forces exerted on both the solid and the porous sphere, also viewed as hydrodynamic correction

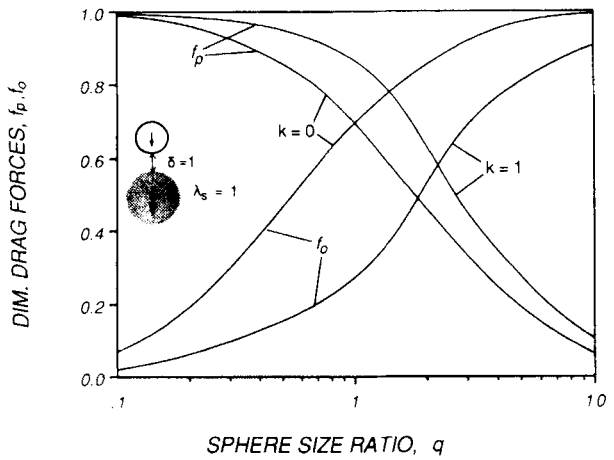

Figure 13. Variation of the drag forces exerted on the solid and on the porous sphere with the sphere size ratio for two permeability values (problem III).

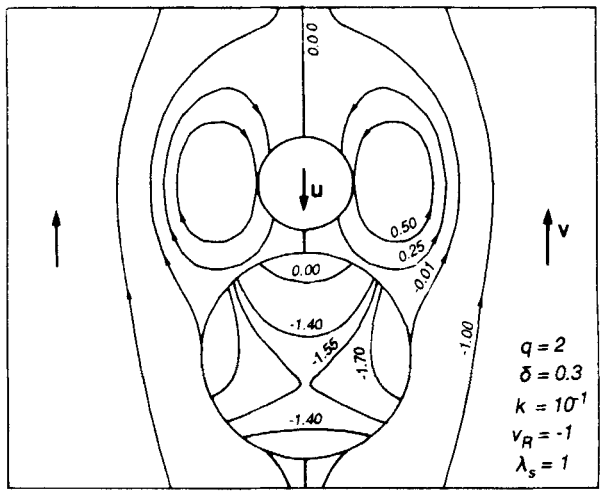

Figure 14. Streamlines and isobars during the combined motion of a solid particle toward a porous sphere and external fluid flow.

factors in this case, are estimated through Eqs. 31 and 32. The value of the drag forces f_p, f_o depends strongly on the permeability, the gap length and the sphere size ratio. The variation of the dimensionless drag force on the solid and on the porous sphere with the gap length for several permeabilities is shown in Figure 12. The two forces point in the same direction. The drag force exerted on the solid sphere exhibits a totally different dependence on the permeability from that of the drag force in problem I. In the present case, it increases monotonically with the gap length for any permeability value, tending to unity for large separations. Another interesting result is that the drag force on the solid particle increases as the permeability of the porous particle increases. This can be explained by the fact that highly permeable spheres allow the fluid to flow through them and fail to "shield" the solid sphere as it is done in the case of two solid spheres. On the other hand, the drag force exerted on the porous particle, f_o, decreases as the gap length decreases for small and moderate permeabilities. For high permeability values the drag force passes through a minimum at finite separations. This slight minimum is more noticeable in Table 3 (for $k=1$). As the permeability decreases the drag force on the porous sphere decreases as in problem I. At large separations our results for the drag force exerted on the porous sphere are in excellent agreement with the results obtained by Neale et al. (1973) for uniform creeping flow past a permeable sphere. As the permeability goes to nil the drag force values determined from our analysis agree with the results of Stimson and Jeffery (1926) for equal spheres, and with the results of Cooley and O'Neill (1969) for arbitrary sphere size ratio and for all the gap lengths considered.

The variation of the drag forces exerted on the solid and porous spheres with the sphere size ratio is shown in Figure 13. For $q>1$, the drag force on the solid particle decreases with increasing q, tending asymptotically to nil for even high permeabilities ($k=1$). The drag on the porous sphere increases with the size of the sphere and tends to unity for $k=0$ and to the solitary porous sphere limit for $k=1$. In the case of porous spheres smaller than the solid particle, the separation distance in Figure 13 is kept equal to the radius of the porous sphere so that it is always equal to the radius of the smaller of the two bodies. It is seen that the effect of the permeability diminishes as the size of the porous sphere decreases; the drag force on the solid particle tends asymptotically to unity whereas that of the porous sphere approaches nil as $q\to 0$.

Flow Around a Solid Sphere Moving Towards a Porous Sphere in an Externally Applied Uniform Flow Field (Composite Problem)

Combining the results of Problems I and II, we can obtain the flow and the pressure field for the case of a solid sphere moving relative to a porous, stationary one in an externally applied uniform flow field. In order to examine a wide range of possible situations, the velocity ratio v_R is used, defined by $\tilde{v}=v_R\tilde{u}$, where $\tilde{u}$ is the constant velocity of the solid sphere and $\tilde{v}$ is the approaching fluid velocity. The stream functions and the pressure values are determined by:

$$\Psi^+ = \Psi_I^+ - v_R\Psi_{II}^+$$

$$P^- = P_I^- - v_R P_{II}^-$$

where subscripts I and II denote quantities in Problem I and II, respectively. The streamlines and the isobars for a typical case are shown in Figure 14. In this case the approach fluid velocity is of equal magnitude with the particle velocity but in the opposite direction ($v_R=-1$). In practice, this situation is mostly observed during upward filtration in packed beds. The opposite directions of particle motion and ambient flow cause generation of quasi-stationary vortices in the neighborhood of the solid particle and very slow motion of fluid within the lower half of the porous obstacle as revealed by the small variation in the indicated pressure values.

The drag forces acting on both spheres can also be obtained. The effect of the velocity ratio v_R on the two drag forces given by:

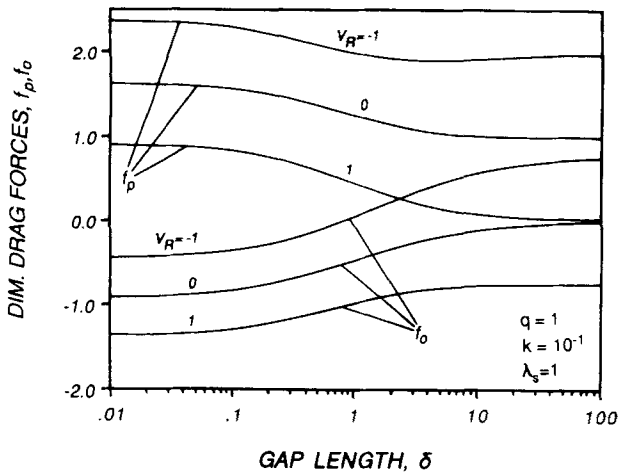

Figure 15. Dependence of the drag forces exerted on the solid and porous spheres on the gap length (composite problem): variation with the velocity ratio (v_R).

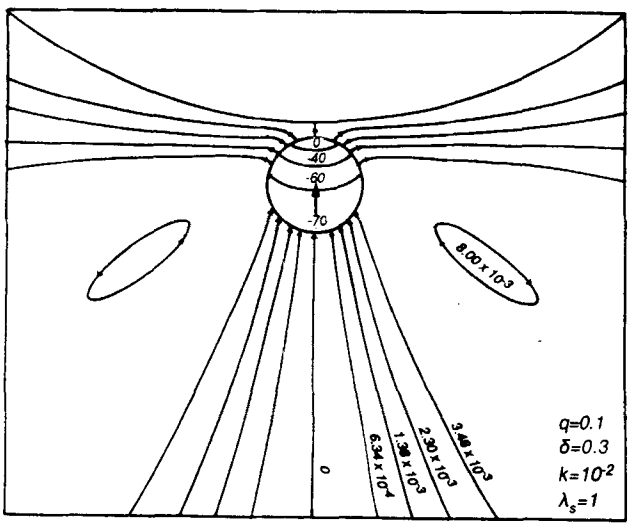

Figure 16. Streamlines and isobars during the motion of a porous particle towards a solid obstacle.

$$f_p = f_{p,\mathrm{I}} - v_R f_{p,\mathrm{II}}$$

$$f_o = f_{o,\mathrm{I}} - v_R f_{o,\mathrm{II}}$$

is depicted in Figure 15, for a relatively high permeability, equal spheres and several gap length values. Quiescent far field is obtained for $v_R = 0$ (problem I). It is seen from this figure that for $v_R = -1$, as the gap length increases the drag force exerted on the solid particle tends to 2, whereas the drag force on the porous particle changes sign. When the two velocities have the same magnitude and direction ($v_R = 1$), no net force on the solid particle is observed for large separations. Further parametric analysis for this composite case can be obtained readily by combining the corresponding results of problems I and II and will be omitted.

Conclusions

The analytical solution to a family of axisymmetric creeping flow problems, where a solid particle and a porous obstacle move relative to each other (or follow each other) in a uniform approach flow field, is obtained using Stokes equation to describe the motion of the fluid in the exterior of the two bodies and Darcy's law in the interior of the porous obstacle. The Beavers-Joseph-Saffman slip condition was employed to describe the tangential flow of the fluid on the porous surface. The flow pattern and the pressure field were determined for each flow problem, and the drag forces exerted on the solid particle and the porous spherical obstacle were calculated. Both drag forces depend strongly on the separation between the two bodies, their relative size, and the permeability of the porous medium. In the case of the composite problem, where the solid particle moves relative to the stationary porous obstacle in an external flow field, the two drag forces are also functions of the relative magnitude and direction of the particle velocity and the approach fluid velocity.

By selecting to solve the two fundamental problems I and III, one becomes able to treat several related flow problems. As an illustration, we show in Figure 16 typical streamlines and isobars for the case of a porous particle moving slowly toward a solid obstacle in a fluid which at infinity is at rest. A limiting case of this problem, namely that of a porous particle moving towards a planar solid wall, was studied by Payatakes and Dassios (1987) and later revised by Burgauos et al. (1992). This problem is directly related to the modeling of deep bed filtration of coagulated particles and of polymer flow through porous media. Extensive analysis of this problem will be presented, as an application, in the future.

Acknowledgment

This work was supported by EC, DG XII, Programme BRITE, Project P-2289, contract No. R11B-0290-C(AM), and by the Institute of Chemical Engineering and High Temperature Chemical Processes.

Notation

a_n = coefficient in Eq. 24
b_n = coefficient in Eq. 24
c = geometric parameter
c_n = coefficient in Eq. 24
d_n = coefficient in Eq. 24
e_n = coefficient in Eq. 26
f_o, f_p = dimensionless drag forces on the solid obstacle and on the porous particle, respectively
$\mathcal{G}_{n+1}(\mu)$ = Gegenbauer polynomial of the first kind, of degree $(-1/2)$ and order n
h = dimensionless distance of the solid particle center to the surface of the porous obstacle ($h = \tilde{h}/\tilde{\alpha}_p = \delta + 1$)
k = dimensionless permeability of the obstacle ($k = \tilde{k}/\tilde{\alpha}_p^2$)
n = outwardly directed normal unit vector
P^+, P^- = dimensionless total pressure in the domains Ω^+ and Ω^-, respectively
$P_n(\mu)$ = Legendre polynomial of the first kind of degree 0 and order n
q = sphere size ratio ($q = \tilde{\alpha}_o/\tilde{\alpha}_p$)
S_o, S_p = surface of the obstacle and of the particle respectively
$\tilde{u}$ = velocity of the solid particle relative to the porous obstacle
$\tilde{v}$ = approach velocity of the fluid
v^+, v^- = dimensionless velocity of the fluid in the domain Ω^+, Ω^-, respectively
$\mathcal{V}_n(\xi)$ = function defined in Eq. 26

v_R = velocity ratio
$\mathcal{W}_n(\xi)$ = function defined in Eq. 24
z = axial cylindrical coordinate

Greek letters

α = geometric parameter
$\tilde{\alpha}_o$ = radius of the porous obstacle
$\tilde{\alpha}_p$ = radius of the solid particle
β = geometric parameter
γ = slip coefficient
δ = dimensionless gap length ($\delta = \tilde{\delta}/\tilde{\alpha}_p$)
λ = tangent unit vector
λ_s = dimensionless slip parameter
μ = bispherical coordinate
$\tilde{\mu}$ = dynamic viscosity
ξ = bispherical coordinate
ρ = dimensionless radial cylindrical coordinate
$\boldsymbol{\rho}$ = unit vector in the $\boldsymbol{\rho}$ direction
τ^+ = dimensionless deviatoric stress tensor
Ψ_I^+, Ψ_{II}^+ = dimensionless Stokes' streamfunction in $\Omega^+(\Psi_I^+ = \tilde{\Psi}_I^+/\tilde{\alpha}_p^2\tilde{u},\ \Psi_{II}^+ = \tilde{\Psi}_{II}^+/\tilde{\alpha}_p^2\tilde{v})$
Ω^+ = domain defined as the exterior of the two spheres
Ω^- = domain defined as the interior of the porous sphere
ω = angle between the unit vectors $\boldsymbol{\rho}$ and $\boldsymbol{\lambda}$

Superscripts

$\sim$ = denotes dimensional quantities
$+$ = denotes quantities in Ω^+
$-$ = denotes quantities in Ω^-

Subscripts

o = denotes quantity related with the porous obstacle
p = denotes quantity related with the solid particle
I, II = denotes quantities in problems I and II, respectively

Literature Cited

Beavers, G. S., and D. D. Joseph, "Boundary Conditions at a Naturally Permeable Wall," *J. Fluid Mech.*, **30**(I), 197 (1967).
Beavers, G. S., E. M. Sparrow, and R. A. Magnuson, "Experiments on Coupled Parallel Flows in a Channel and a Bounding Porous Medium," *J. Basic Eng., Trans. ASME*, Series D, **92**, 843 (1970).
Brenner, H., "The Slow Motion of a Sphere Through a Viscous Fluid Towards a Plane Surface," *Chem. Eng. Sci.*, **16**, 242 (1961).
Burgauos, V. N, A. C. Michalopaulos, G. Dassios, and A. C. Payatakes, "Creeping Flow around and through a Permeable Sphere Moving with Constant Velocity towards a Solid Wall: A Revision," *Chem. Eng. Commun.*, in press (1992).
Cooley, M. D. A., and M. E. O'Neill, "On the Slow Motion Generated in a Viscous Fluid by the Approach of a Sphere to a Plane Wall or Stationary Sphere," *Mathematika*, **16**, 37 (1969).
Cooley, M. D. A., and M. E. O'Neill, "On the Slow Motion of Two Spheres in Contact Along Their Line of Centers in a Viscous Fluid," *Proc. Cambridge Phil. Soc.*, **66**, 407 (1969).
Dean, W. R., and M. E. O'Neill, "A Slow Motion of Viscous Liquid Caused by the Rotation of a Solid Sphere," *Mathematika*, **10**, 13 (1963).
Goldman, A. J., R. G. Cox, and H. Brenner, "The Slow Motion of Two Identical Arbitrarily Oriented Spheres Through a Viscous Fluid," *Chem. Eng. Sci.*, **21**, 1151 (1966).
Goldman, A. J., R. G. Cox, and H. Brenner, "Slow Viscous Motion of a Sphere Parallel to a Plane Wall. -I Motion Through a Quiescent Fluid," *Chem. Eng. Sci.*, **22**, 637 (1967a).
Goldman, A. J., R. G. Cox, and H. Brenner, "Slow Viscous Motion of a Sphere Parallel to a Plane Wall.-II Couette Flow," *Chem. Eng. Sci.*, **22**, 653 (1967b).
Goren, S. L., and M. E. O'Neill, "On the Hydrodynamic Resistance to a Particle of a Dilute Suspension when in the Neighborhood of a Large Obstacle," *Chem. Eng. Sci.*, **26**, 325 (1971).
Goren, S. L., "The Hydrodynamic Force Resisting the Approach of a Sphere to a Plane Permeable Wall," *J. Coll. and Int. Sci.*, **69**(1), 78 (1979).
Happel, J., and H. Brenner, *Low Reynolds Number Hydrodynamics*, Martinus Nijhoff Publishers, Dordrecht (1983).
Hobson, E. W., *The Theory of Spherical and Ellipsoidal Harmonics*, Chelsea Publishing Company, New York (1965).
Jones, R. B., "Hydrodynamic Interaction of Two Permeable Spheres I: The Method of Reflections," *Physica*, **92A**, 545 (1978).
Jones, R. B., "Hydrodynamic Interaction of Two Permeable Spheres II: Velocity Field and Friction Constants," *Physica*, **92A**, 557 (1978).
Jones, R. B., "Hydrodynamic Interaction of Two Permeable Spheres III: Mobility Tensors," *Physica*, **92A**, 571 (1978).
Kynch, G. J., "The Slow Motion of Two or More Spheres Through a Viscous Fluid," *J. Fluid Mech.*, **5**, 193 (1958).
Maude, A. D., "End Effects in a Falling-Sphere Viscometer," *Br. J. Appl. Physics*, **12**, 293 (1961).
Morse, P. M., and H. Feshbach, *Methods of Theoretical Physics*, Vol. II, McGraw Hill, New York (1953).
Neale, G., N. Epstein, and W. Nader, "Creeping Flow Relative to Permeable Spheres," *Chem. Eng. Sci.*, **28**, 1865 (1973).
Neale, G., and W. Nader, "Practical Significance of Brinkman's Extension of Darcy's Law: Coupled Parallel Flows with a Channel and a Bounding Porous Medium," *Can. J. of Chem. Eng.*, **52**, 475 (1974).
Nir, A., "On the Departure of a Sphere from Contact with a Permeable Membrane," *J. Eng. Math.*, **15**(1), 65 (1981).
O'Neill, M. E., and B. S. Bhatt, "Slow Motion of a Solid Sphere in the Presence of a Naturally Permeable Surface," *Q. Jl. Mech. Appl. Math.*, **44**(1), 91 (1991).
Payatakes, A. C., and G. Dassios, "Creeping Flow Around and Through a Permeable Sphere Moving with Constant Velocity Towards a Solid Wall," *Chem. Eng. Com.*, **58**, 119 (1987).
Payne, L. E., and W. H. Pell, "The Stokes Flow Problem for a Class of Axially Symmetric Bodies," *Fluid Mech.*, **7**, 529 (1959).
Richardson, S., "A Model for the Boundary Condition of a Porous Material. Part 2," *J. Fluid Mech.*, **49**(2), 327 (1971).
Saffman, P. G., "On the Boundary Condition at the Surface of a Porous Medium," *St. Appl. Math.*, **L**(2), 93 (1971).
Sherwood, J. D., "The Force on a Sphere Pulled Away from a Permeable Half-Space," *PCH*, **10**(1), 3 (1988).
Stimson, M., and G. B. Jeffery, "The Motion of Two Spheres in a Viscous Fluid," *Proc. Roy. Soc.*, **A111**, 110 (1926).
Taylor, G. I., "A Model for the Boundary Condition of a Porous Material. Part I," *J. Fluid Mech.*, **49**(2), 319 (1971).
Yang, S., and L. G. Leal, "Motion of a Porous Particle in Stokes Flow Near a Plane-Fluid Interface," *PCH*, **11**(4), 543 (1989).

Appendix A: Final Form of the Boundary Conditions on the Porous Sphere (Problem I)

The boundary condition, Eq. 19, yields:

$$\sum_{i=1}^{\lambda_\kappa} A_i(\kappa - i) = 0; \quad \kappa = 3,\ 4,\ 5,\ \ldots$$

where, $\lambda_3 = 3$, $\lambda_4 = 4$, $\lambda_\kappa = 5$ for $\kappa \geq 5$ and

$$A_1(n) = -kc\mathcal{V}_n'(\beta)\delta_{2,-2}^n$$

$$A_2(n) = \left[\frac{3}{2(2n+1)} + \delta_{1,-1}^n\right]\mathcal{W}_n(\beta) + kc\left[\frac{s}{2}\mathcal{V}_n(\beta) + 2t\mathcal{V}_n'(\beta)\right]\delta_{1,-1}^n$$

$$A_3(n) = -tW_n(\beta) - kc\left[\frac{st}{2}\mathcal{V}_n(\beta) + (t^2 + \delta_{2,0}^n)\mathcal{V}_n'(\beta)\right]$$

$$A_4(n)=\left(\delta^n_{1,1}-\frac{3}{2(2n+1)}\right)\mathcal{W}_n(\beta)+kc\left[\frac{s}{2}\,\mathcal{V}_n(\beta)+2t\mathcal{V}_n'(\beta)\delta^n_{1,1}\right]$$

$$A_5(n)=-kc\mathcal{V}_n'(\beta)\delta^n_{2,2}$$

$$\delta^n_{i,j}\equiv\delta_{i,j}(n)$$

with $s\equiv\sinh\beta$ and $t\equiv\cosh\beta$.
The prime denotes differentiation with respect to ξ, and $\delta_{i,j}{}^n$ are expressions defined in the following property of Legendre polynomials (see Hobson, 1965, p. 45)

$$\mu^\kappa P_n(\mu)=\sum_{i=0}^{\kappa}\delta^n_{\kappa,\,\kappa+2i}P_{n-\kappa+2i}(\mu)$$

For instance, for $\kappa=1$ we obtain

$$\mu P_n(\mu)=\delta^n_{1,-1}P_{n-1}+\delta^n_{1,1}P_{n+1}=\frac{n}{2n+1}\,P_{n-1}+\frac{n+1}{2n+1}\,P_{n+1}$$

The boundary condition, Eq. 20 yields:

$$\sum_{i=1}^{\lambda_\kappa}B_i(\kappa-i)=0;\quad \kappa=4,5,6,\ \ldots$$

where $\lambda_4=3$, $\lambda_5=4$, $\lambda_6=5$, $\lambda_7=6$, $\lambda_\kappa=7$ for $\kappa\geq 8$, and

$$B_1(n)=C_2(n)\delta^{n-1}_{2,-2}$$

$$B_2(n)=C_1(n)\delta^{n-1}_{1,-1}$$

$$B_3(n)=C_0(n)+C_2(n)\delta^{n-1}_{2,0}-C_2(n)\delta^{n+1}_{2,-2}$$

$$B_4(n)=C_1(n)\delta^{n-1}_{1,1}-C_1(n)\delta^{n+1}_{1,-1}$$

$$B_5(n)=-C_0(n)+C_2(n)\,(\delta^{n-1}_{2,2}-\delta^{n+1}_{2,0})$$

$$B_6(n)=-C_1(n)\delta^{n+1}_{1,1}$$

$$B_7(n)=-C_2(n)\delta^{n+1}_{2,2}$$

$$C_0(n)=\left[-\frac{3}{2}\,(\gamma c-3s)s-\frac{3}{4}-\frac{15}{4}\,s^2+\frac{3}{2}\,t^2-t^2\,n(n+1)\right]\mathcal{W}_n(\beta)+[(\gamma c-3s)t+3t]\mathcal{W}_n'(\beta)-t^2\mathcal{W}_n''(\beta)$$

$$C_1(n)=-\frac{3t}{2}\,\mathcal{W}_n(\beta)-(\gamma c-3s)\mathcal{W}_n'(\beta)-3s\mathcal{W}_n'(\beta)+2t\,n(n+1)\mathcal{W}_n(\beta)+2t\mathcal{W}_n''(\beta)$$

$$C_2(n)=\frac{3}{4}\,\mathcal{W}_n(\beta)-n(n+1)\mathcal{W}_n(\beta)-\mathcal{W}_n''(\beta)$$

Finally, the boundary condition, Eq. 18, gives

$$\sum_{i=1}^{\lambda_\kappa}D_i(\kappa-i)=0;\quad \kappa=5,\ 6,\ 7,\ \ldots$$

where $\lambda_5=5$, $\lambda_6=6$, $\lambda_7=7$, $\lambda_8=8$, $\lambda_\kappa=9$ for $\kappa\geq 9$, and

$$D_1(n)=\frac{1}{2n+1}\,E_3(n)\delta^{n-1}_{3,-3}+F_4(n)\delta^n_{4,-4}$$

$$D_2(n)=\frac{1}{2n+1}\,E_2(n)\delta^{n-1}_{2,-2}+F_3(n)\delta^n_{3,-3}+\left[\frac{1}{2}\,\delta^n_{3,-3}-\frac{n(n+1)}{2n+1}\,\delta^{n-1}_{2,-2}\right]c^3\mathcal{V}_n(\beta)$$

$$D_3(n)=\frac{1}{2n+1}\left[E_1(n)\delta^{n-1}_{1,-1}+(\delta^{n-1}_{3,-1}-\delta^{n-1}_{3,-3})E_3(n)\right]+F_2(n)\delta^n_{2,-2}+F_4(n)\delta^n_{4,-2}+\left[-\frac{1}{2}\,\delta^n_{2,-2}+2\,\frac{n(n+1)}{2n+1}\,\delta^{n-1}_{1,-1}\right]c^3t\mathcal{V}_n(\beta)$$

$$D_4(n)=\frac{1}{2n+1}\left[E_0(n)+(\delta^{n-1}_{2,0}-\delta^{n+1}_{2,-2})E_2(n)\right]+F_1(n)\delta^n_{1,-1}+F_3(n)\delta^n_{3,-1}+\left[\frac{1}{2}\,\delta^n_{1,-1}+\frac{1}{2}\,\delta^n_{3,-1}-\frac{n(n+1)}{2n+1}\,(t^2+\delta^{n-1}_{2,0}-\delta^{n+1}_{2,0})\right]c^3\mathcal{V}_n(\beta)$$

$$D_8(n)=-\frac{1}{2n+1}\,E_2(n)\delta^{n+1}_{2,2}+F_3(n)\delta^n_{3,3}+\left[\frac{1}{2}\,\delta^n_{3,3}+\frac{n(n+1)}{2n+1}\,\delta^{n+1}_{2,2}\right]c^3\mathcal{V}_n(\beta)$$

$$D_9(n)=-\frac{1}{2n+1}\,E_3(n)\delta^{n+1}_{3,3}+F_4(n)\delta^n_{4,4}$$

$$E_0(n)=\left[\frac{3}{8}-\frac{1}{2}\,n(n+1)\right]st^2\mathcal{W}_n(\beta)+\left[\frac{5}{4}\,t-\frac{5}{2}\,t^3+\frac{9}{4}\,ts^2-t^3n(n+1)\right]\mathcal{W}_n'(\beta)-\frac{3}{2}\,t^2\,s\mathcal{W}_n''(\beta)+t^3\mathcal{W}_n'''(\beta)$$

$$E_1(n)=\left[-\frac{9}{4}+n(n+1)\right]st\mathcal{W}_n(\beta)+\left[6t^2-\frac{5}{4}-\frac{9}{4}\,s^2+3t^2\,n(n+1)\right]\mathcal{W}_n'(\beta)+3st\mathcal{W}_n''(\beta)-3t^2\mathcal{W}_n'''(\beta)$$

$$E_2(n)=\left[\frac{15}{8}-\frac{1}{2}\,n(n+1)\right]s\mathcal{W}_n(\beta)+\left[-\frac{23}{4}-3n(n+1)\right]t\mathcal{W}_n'(\beta)-\frac{3}{2}\,s\mathcal{W}_n''(\beta)+3t\mathcal{W}_n'''(\beta)$$

$$E_3(n)=\left[\frac{9}{4}+n(n+1)\right]\mathcal{W}_n'(\beta)-\mathcal{W}_n'''(\beta)$$

$$F_0(n)=ts\mathcal{W}_n(\beta)-2t^2\mathcal{W}_n'(\beta)$$

$$F_1(n) = -s\mathfrak{W}_n(\beta) + 4t\mathfrak{W}_n'(\beta)$$

$$F_2(n) = -ts\mathfrak{W}_n(\beta) - 2\mathfrak{W}_n'(\beta) + 2t^2\mathfrak{W}_n'(\beta)$$

$$F_3(n) = s\mathfrak{W}_n(\beta) - 4t\mathfrak{W}_n'(\beta), \quad F_4(n) = 2\mathfrak{W}_n'(\beta)$$

Appendix B: Final Form of the Boundary Conditions on the Porous Sphere (Problem II)

The boundary condition, Eq. 33, gives:

$$\sum_{i=1}^{\lambda_\kappa} A_i(\kappa - i)$$

$$= c^2\sqrt{2} \sum_{n=0}^{\infty} \left[-e^{(n+1/2)\beta} + t\,\frac{(n+1)}{2n+3}\,e^{(n+3/2)\beta} + t\,\frac{n}{2n-1}\,e^{(n-1/2)\beta} \right]$$

for $\kappa = 3,4,5, \ldots$

where $\lambda_3 = 3$, $\lambda_4 = 4$, $\lambda_\kappa = 5$ for $\kappa \geq 5$
The functions $Ai(n)$ are given in Appendix A.
Finally, the boundary condition, Eq. 34 gives:

$$\sum_{i=1}^{\lambda_\kappa} B(\kappa - i) = \gamma c^3 s\,\frac{\sqrt{2}}{2} \sum_{n=1}^{\infty} n(n+1) \left[\frac{e^{(n-1/2)\beta}}{(n-1/2)} - \frac{e^{(n+3/2)\beta}}{(n+3/2)} \right]$$

for $\kappa = 4, 5, 6, \ldots$
where $\lambda_4 = 3$, $\lambda_5 = 4$, $\lambda_6 = 5$, $\lambda_7 = 6$, $\lambda_\kappa = 7$ for $\kappa \geq 8$
The functions $Bi(n)$ are given in Appendix A.

Manuscript received Feb. 7, 1992, and revision received Apr. 21, 1992.